

# Strangeness Production at COSY

Frank Hinterberger\*, Hartmut Machner† and Regina Siudak\*\*

\*HISKP, Universität Bonn, Nussallee 14-16, D 53115 Bonn, Germany

†Fakultät für Physik, Universität Duisburg-Essen, Lotharstr. 1, D 47048 Duisburg, Germany

\*\*Inst. Nucl. Physics, PAN, ul. Radzikowskiego 152, 31-342 Kraków, Poland

**Abstract.** The paper gives an overview of strangeness-production experiments at the Cooler Synchrotron COSY. Results on kaon-pair and  $\phi$  meson production in  $pp$ ,  $pd$  and  $dd$  collisions, hyperon-production experiments and  $\Lambda p$  final-state interaction studies are presented.

**Keywords:** Associated strangeness production, Final state interactions, Hyperon-nucleon interactions

**PACS:** 13.75.Cs, 13.75.-n, 14.20.Jn, 14.40.Df, 14.20.Jn 25.40.Ve

## INTRODUCTION

The cooler synchrotron COSY [1] at the Forschungszentrum Jülich in Germany can accelerate protons and deuterons up to about 3.7 GeV/c. Both, unpolarized and polarized beams are available. Excellent beam quality can be achieved using electron- and/or stochastic cooling. COSY can be used as an accelerator for external target experiments and as storage ring for internal target experiments. The strangeness production experiments have been performed at the internal spectrometer ANKE by the COSY-ANKE collaboration, at the internal COSY-11 spectrometer by the COSY-11 collaboration, at the external TOF facility by the COSY-TOF collaboration and at the external BIG KARL spectrometer by the COSY-MOMO and COSY-HIRES collaborations.

## KAON-PAIR PRODUCTION EXPERIMENTS

Extensive measurements of kaon-pair production have been performed at several COSY facilities. Total and differential cross sections are now available for a variety of reactions. The world data set of total cross sections for kaon pair production is shown in Fig. 1, left panel, as a function of the excess energy  $\varepsilon$ . The  $pp \rightarrow ppK^+K^-$  reaction (black symbols) has been studied by the COSY-11 [2, 3, 4] and COSY-ANKE [5, 6] collaborations at excitation energies between 3 and 108 MeV. The closely related reaction  $pp \rightarrow dK^+\bar{K}^0$  (green) has also been studied by COSY-ANKE [7, 8]. In addition the reaction  $pn \rightarrow dK^+K^-$  (red) has been investigated by COSY-ANKE [9, 10] using a deuterium cluster-jet as neutron target. The momentum of the non-observed proton spectator and the excess energy  $\varepsilon$  have been reconstructed from the four-momenta of the detected deuteron and kaon pair. The  $pd \rightarrow {}^3\text{He}K^+K^-$  (pink) reaction has been measured by the COSY-MOMO collaboration [11]. The  $dd \rightarrow {}^4\text{He}K^+K^-$  reaction studied by COSY-ANKE is an ideal isospin zero filter. It could be sensitive to the production of the scalar meson  $f_0(980)$ . But the total cross section (blue point) amounts only to 5 pb [12]. The high energy  $pp \rightarrow ppK^+K^-$  result (open circle) has been measured at SATURNE [13].

The invariant mass distribution of  $K^+K^-$  pairs has been measured by COSY-ANKE [6] at three excess energies  $\varepsilon = 51, 67$  and 108 MeV. The internal ANKE spectrometer detects simultaneously slow positive and negative particles in the side detectors and fast positive particles in the forward detector. The spectrum taken at  $\varepsilon = 51$  MeV ( $T_p = 2.65$  GeV) is shown in Fig. 1, right panel. All three spectra show a strong peak which is due to the production of the  $\phi(1020)$  meson which decays with about 50 % into  $K^+K^-$ . The prompt  $K^+K^-$  distribution can be described by a 4-body phase-space distribution modified by the  $pp$  and  $K^-p$  final state interaction (FSI). All three distributions show a low mass enhancement over the fit curves. This enhancement has been discussed as a coupled channel effect due to the  $K^0\bar{K}^0$  channel whose threshold (dashed vertical line) is about 8 MeV above the  $K^+K^-$  threshold [14].

The important  $K^-p$  FSI has been observed by comparing the invariant mass distributions of  $K^-p$  and  $K^+p$  [6, 15]. The ratio of  $K^-p$  to  $K^+p$  production changes by an order of magnitude within 50 MeV. The same holds true if one compares  $K^-pp$  and  $K^+pp$ . The  $K^-p$  FSI can be described by assuming an imaginary scattering length of 1.5 fm.

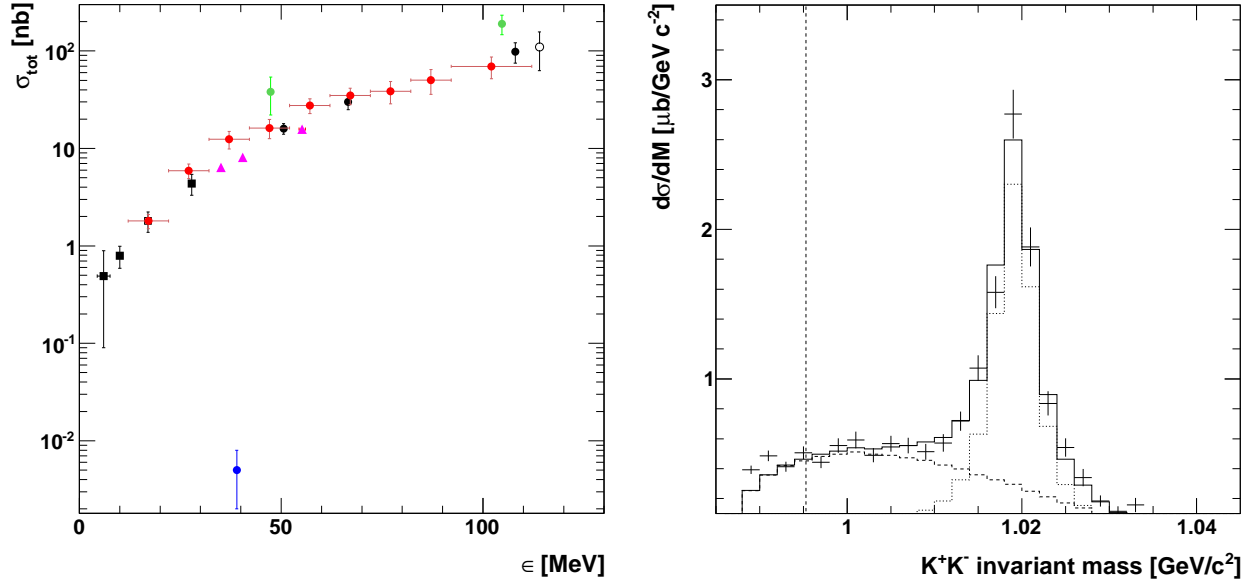


**FIGURE 1.** Left: Total cross sections for kaon-pair production as a function of the excess energy  $\epsilon$  measured at COSY. Black:  $pp \rightarrow ppK^+K^-$  [2, 3, 4, 5, 6]. Green:  $pp \rightarrow dK^+K^0$  [7, 8]. Red:  $pn \rightarrow dK^+K^-$  [9, 10]. Pink:  $pd \rightarrow {}^3\text{He}K^+K^-$  [11]. Blue:  $dd \rightarrow {}^4\text{He}K^+K^-$  [12]. The high energy  $pp \rightarrow ppK^+K^-$  result (open circle) has been measured at SATURNE [13]. Right: Invariant mass distribution of  $K^+K^-$  pairs measured by COSY-ANKE [6] at  $\epsilon = 51$  MeV ( $T_p = 2.65$  GeV). Dotted and dashed histograms represent the  $\phi$  and non- $\phi$  contributions. The solid histogram is the sum of both. The  $K^0\bar{K}^0$  threshold is indicated by the dashed vertical line.

In Fig. 2, the left panel shows the total cross sections for  $pp \rightarrow ppK^+K^-$  as a function of the excess energy  $\epsilon$ . The data are from COSY-11 [2, 3, 4], COSY-ANKE [5, 6] and SATURNE-DISTO [13]. The dashed curve represents a pure 4-body phase-space calculation. The dot-dashed curve includes the  $pp$  FSI and the solid curve includes the  $K^-p$  FSI. The right panel shows the total cross section for  $\phi$  production as a function of the corresponding excess energy  $\epsilon$ . The data cannot be described by a pure three-body phase-space behavior. But the inclusion of the  $pp$  FSI is

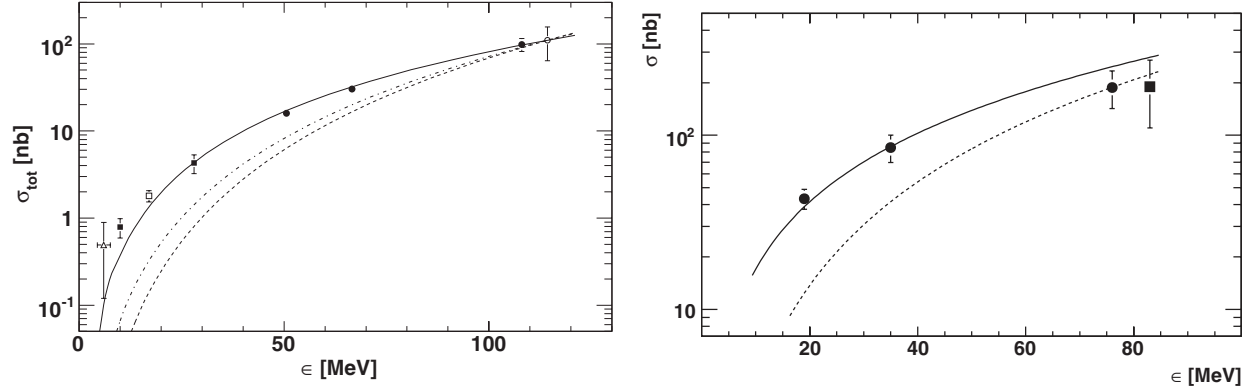


**FIGURE 2.** Left: Total cross section for  $pp \rightarrow ppK^+K^-$  vs. excess energy  $\epsilon$  [6]. Data from COSY-ANKE (closed circles) [6], COSY-11 (open triangle) [2], (open square) [3], (closed squares) [4] and DISTO (open circle) [13]. The dashed curve represents the energy dependence from four-body phase space. The dot-dashed includes the  $pp$  FSI and the solid curve includes the  $K^-p$  FSI. Right: Total cross sections for  $pp \rightarrow pp\phi$  vs. excess energy  $\epsilon$  [5]. Data from COSY-ANKE (closed circles) [5] and DISTO (closed square) [13]. The dashed curve represents a three-body phase-space calculation. The solid curve includes the  $pp$  FSI.

sufficient to reproduce the energy dependence [5]. Another important result is the angular distribution of the  $\phi$  decay into  $K^+K^-$  at  $\epsilon = 18.5$  MeV which is a pure  $\sin^2 \Theta$  distribution in the Jackson frame. Thus, the  $\phi$  meson is tensor polarized with  $m = \pm 1$  along the beam axis as expected near threshold due to conservation laws [5]. Comparing the

total cross sections for  $\phi$ - and  $\omega$ -production at corresponding excess energies [5, 16] yields a ratio  $R_{\phi/\omega}$  which is about eight times larger than the prediction  $R_{OZI} = 4.2 \cdot 10^{-3}$  [17] based on the Okubo-Zweig-Iizuka (OZI) rule.

The  $K^+K^-$ - and  $\phi$ -production was also studied by the COSY-MOMO collaboration at the magnetic spectrograph BIG KARL using the  $pd \rightarrow {}^3\text{He}K^+K^-$  reaction [11]. The invariant mass distributions measured at three excess energies, 35, 40 and 55 MeV, can be described by pure phase-space distributions. Effects due to a possible  $K^-{}^3\text{He}$  FSI are not visible. In comparison to the  $pp \rightarrow pp\phi$  reaction [5] the  $\phi$  peak is less pronounced. The surprising result of the  $pd \rightarrow {}^3\text{He}\phi$  study is that the  $\phi$  meson is tensor polarized with  $m = 0$  along the beam axis [11]. In contrast, the  $\omega$  meson is unpolarized in the corresponding reaction  $pd \rightarrow {}^3\text{He}\omega$  [18]. The ratio  $R_{\phi/\omega}$  of total cross sections for  $pd \rightarrow {}^3\text{He}\phi$  and  $pd \rightarrow {}^3\text{He}\omega$  at corresponding excess energies is about a factor 20 larger [11] than predicted by the OZI-rule [17].

## HYPERON-PRODUCTION EXPERIMENTS

Exclusive measurements of hyperon production have been performed using the associated strangeness reactions  $pp \rightarrow K^+\Lambda p$ ,  $pp \rightarrow K^+\Sigma^0 p$ ,  $pp \rightarrow K^+\Sigma^+ n$  and  $pp \rightarrow K^0\Sigma^+ p$  by the COSY-11, COSY-ANKE and COSY-TOF collaborations. The aim of those measurements is to understand (i) the reaction mechanism, (ii) to study the effect of  $N^*$  resonances and (iii) to study the FSI between the outgoing nucleon and hyperon.

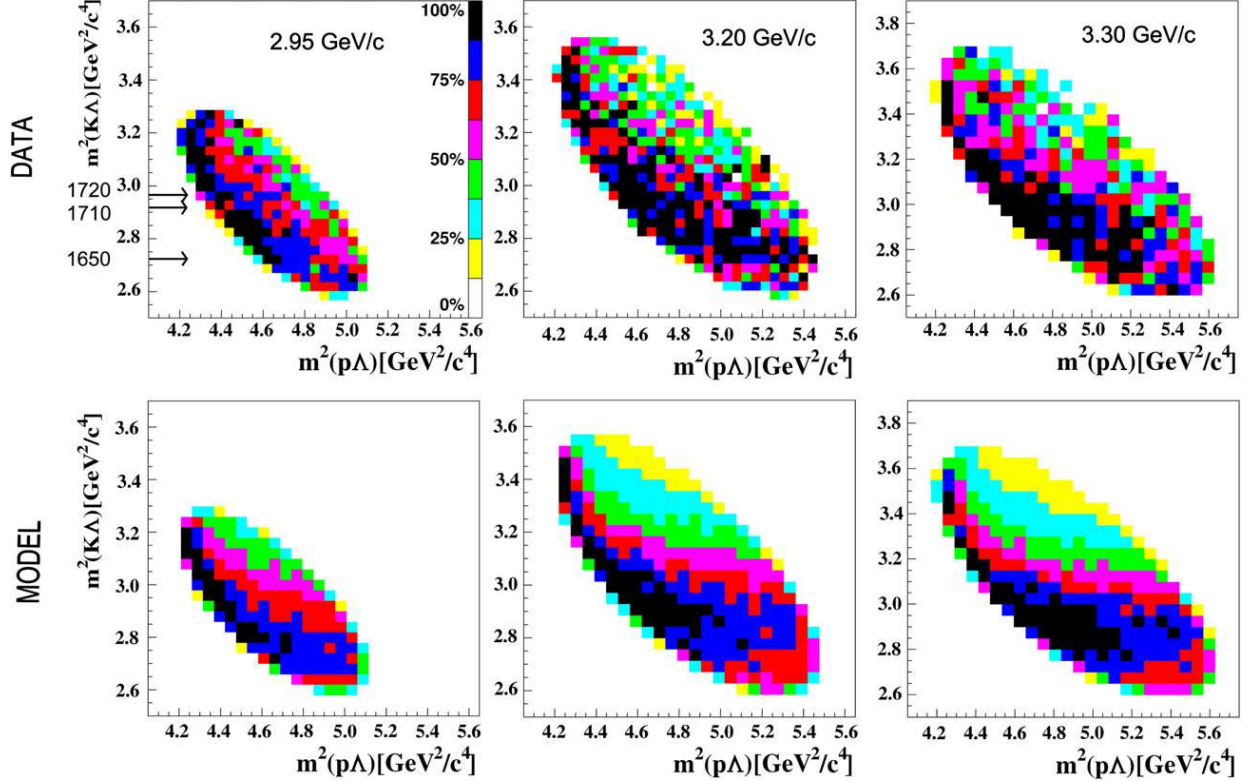


**FIGURE 3.** Dalitz plots of the reaction  $pp \rightarrow K^+\Lambda p$  measured by COSY-TOF at 2.95, 3.20 and 3.30 GeV/c [19]. The model calculations are performed using the ISOBAR model of Sibirtsev [20].

The COSY-TOF detector enables exclusive measurements with a large solid angle in the laboratory system and almost  $4\pi$  in the c.m. system. Recent measurements of the reaction  $pp \rightarrow K^+\Lambda p$  at three bombarding energies [19] are shown in Fig. 3 in the form of Dalitz plots. The Dalitz plots show strong deviations from a homogeneous phase-space distribution. The data can be described using the ISOBAR model of Sibirtsev (concept outlined in [20]) which takes into account the  $\Lambda p$  FSI and the contribution of three  $N^*$  resonances,  $N(1650)$ ,  $N(1710)$  and  $N(1720)$ . The exclusive measurements of  $pp \rightarrow K^+\Lambda p$  and  $pp \rightarrow K^+\Sigma^0 p$  by COSY-TOF provide also differential cross sections [21] in the

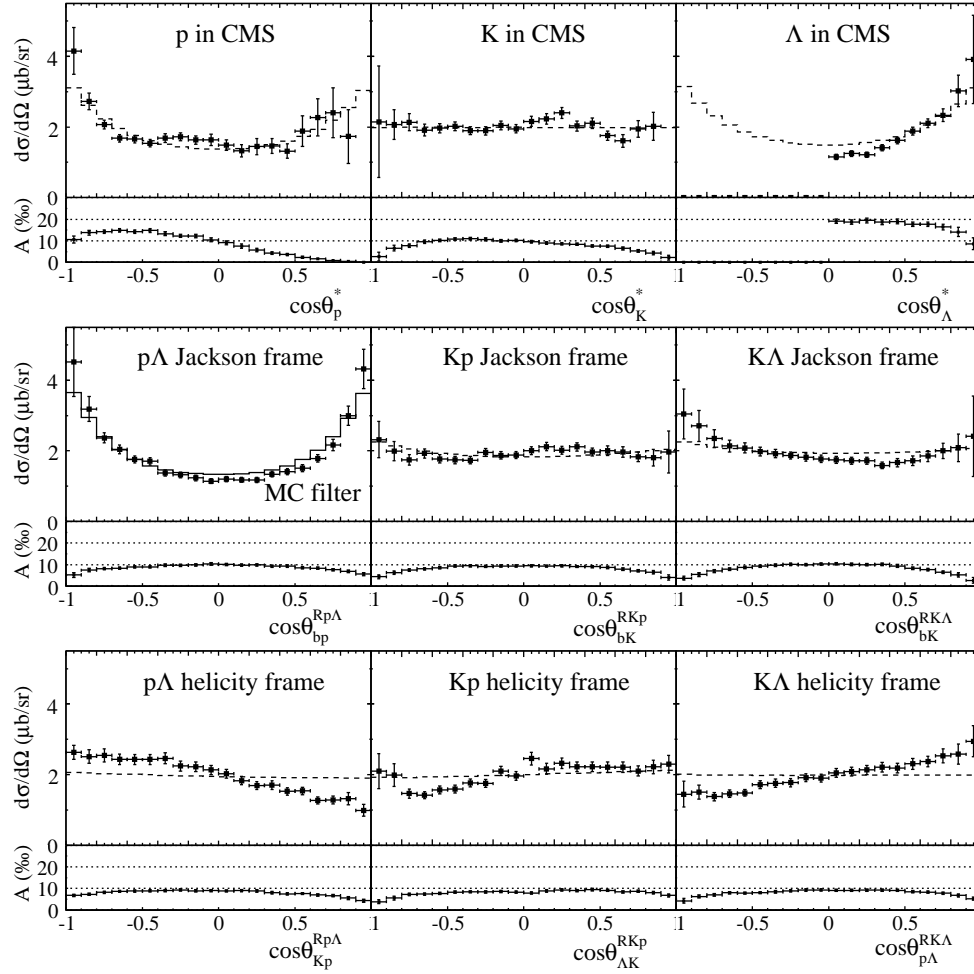


**FIGURE 4.** Differential cross sections in the CMS, Jackson and helicity frames for the reaction  $pp \rightarrow K^+\Lambda p$  measured by COSY-TOF at  $p_{beam} = 3.059$  GeV/c [21]. Note the differential acceptances  $A(\%)$ .

CMS, Jackson and helicity frames, see Fig. 4. In addition, first measurements with polarized proton beams have been performed. The COSY-TOF data will be used for a detailed partial wave analysis by the Bonn-Gatchina PWA group.

In Fig. 5 [21] the total cross sections for  $pp \rightarrow K^+\Lambda p$  and  $pp \rightarrow K^+\Sigma^0 p$  [21, 22, 23, 24, 25, 26, 27, 28, 29] are shown as a function of the corresponding excess energy  $\epsilon$ . The dashed curves representing a three-body phase-space  $\epsilon^2$  dependence describe the  $pp \rightarrow K^+\Sigma^0 p$  data and there is no evidence for a  $\Sigma^0 p$  FSI. However, the  $pp \rightarrow K^+\Lambda p$  data can only be described by including the  $\Lambda p$  FSI. The right panel shows the ratio of the  $pp \rightarrow K^+\Lambda p$  to  $pp \rightarrow K^+\Sigma^0 p$  total cross sections as a function of the excess energy. The new experimental values from COSY-TOF [21] confirm the general trend towards a ratio of 2.2 measured at high energies [30]. The large increase of the ratio towards low energies is well described by the  $\Lambda p$  FSI.

The first measurement of the reaction  $pp \rightarrow K^+\Sigma^+ n$  close to threshold has been performed by COSY-11 [31], by detecting the  $K^+$  in coincidence with the neutron. The total cross sections at  $\epsilon = 13$  and 60 MeV were astonishingly high compared to those for  $pp \rightarrow K^+\Sigma^0 p$ . Therefore, the energy dependence of the reaction  $pp \rightarrow K^+\Sigma^+ n$  close to threshold has been studied recently by COSY-ANKE [28, 32] by detecting  $K^+$  in coincidence with  $\pi^+$  from the decay of the  $\Sigma^+$  and by detecting  $K^+ p$  coincidences. In contrast to the COSY-11 results [31] the total cross sections for  $pp \rightarrow K^+\Sigma^+ n$  are very much smaller (factor 50 at  $\epsilon = 60$  MeV) and slightly smaller than those for  $pp \rightarrow K^+\Sigma^0 p$  ( $R(\Sigma^+/\Sigma^0) = 0.7 \pm 0.1$ ). The energy dependence can be described by a three-body phase-space calculation [32], with no evidence for a  $\Sigma^+ n$  FSI. Details can be found in the contribution of Yu. Valdau to these proceedings.

A recent determination of the total cross section for  $pp \rightarrow K^+\Sigma^+ n$  at  $\epsilon = 102.6$  MeV from inclusive  $K^+$  data by

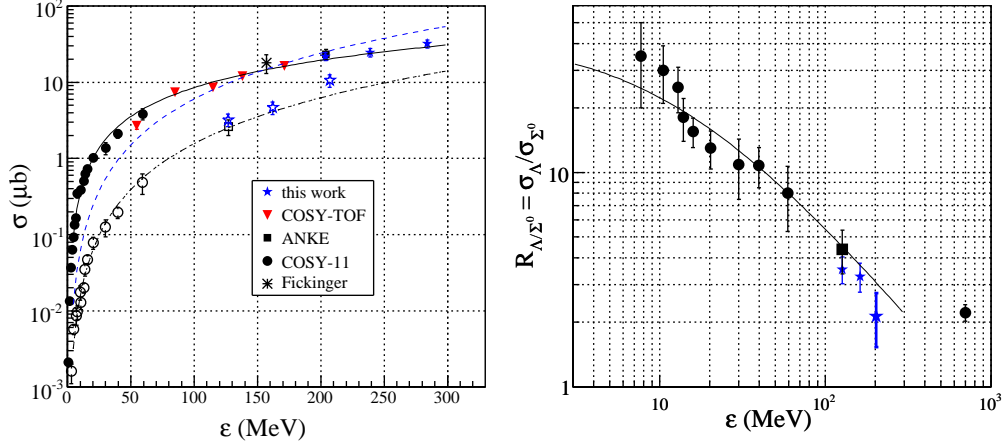


**FIGURE 5.** Left: Total cross sections for  $pp \rightarrow K^+\Lambda p$  (solid symbols) and  $pp \rightarrow K^+\Sigma^0 p$  (open symbols) [21, 22, 23, 24, 25, 26, 27, 28, 29] vs. corresponding excess energy  $\varepsilon$ . The new data (open and solid crosses, denoted 'this work' in the insert) are from COSY-TOF [21]. The dashed curves represent a three-body phase-space  $\varepsilon^2$  dependence. The solid curve includes the  $\Lambda p$  FSI. Right: Ratio of the  $pp \rightarrow K^+\Lambda p$  to  $pp \rightarrow K^+\Sigma^0 p$  total cross sections vs.  $\varepsilon$ . The ratio at  $\varepsilon = 700$  MeV is an average value calculated from data given in [30]. The solid curve takes the  $\Lambda p$  FSI into account.

COSY-HIRES [33] yielded also a value smaller than expected from the COSY-11 results. But the result is in conflict with the exclusive measurement by COSY-ANKE [28, 32]. Possible reasons for this discrepancy are discussed in [34].

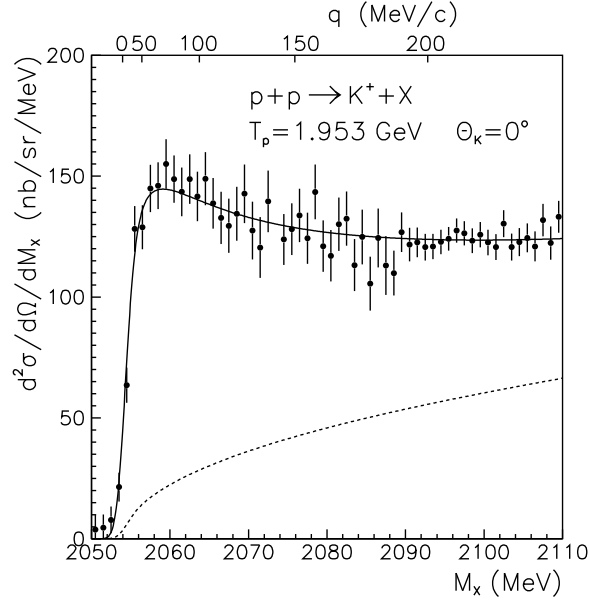


**FIGURE 6.** Missing mass spectrum of the reaction  $pp \rightarrow K^+\Lambda p$  measured at  $T_p = 1.953$  GeV and  $\Theta_K = 0^\circ$  [35]. Solid curve: fit with spin-averaged effective range parameters. Dashed curve: phase-space distribution.

The  $\Lambda p$  FSI in the reaction  $pp \rightarrow K^+\Lambda p$  has been studied with a high invariant mass resolution by the COSY-HIRES collaboration [35]. The kaons were detected at  $0^\circ$  using the magnetic spectrograph BIG KARL [36]. The double differential cross section is shown in Fig. 6 as a function of the missing mass, i.e. the invariant mass of the  $\Lambda p$  system. The spectrum is characterized by a huge FSI enhancement near the  $\Lambda p$  threshold. A narrow  $S = -1$  dibaryon resonance predicted near 2100 MeV [37] is not visible. The data can be described by factorizing the reaction amplitude in terms of a production amplitude and a FSI enhancement factor (solid curve in Fig. 6). Taking for the enhancement the

inverse Jost function yields the spin-averaged effective range parameters of the  $\Lambda p$  interaction, i.e. the scattering length  $\bar{a} = -2.43^{+0.16}_{-0.17}$  fm and the effective range  $\bar{r} = 2.21 \pm 0.16$  fm. The dashed curve is the corresponding phase-space distribution without FSI enhancement. Taking the free  $\Lambda p$  scattering data [38, 39] in a combined fit into account yields the possibility to disentangle the spin singlet and triplet effective range parameters of the  $\Lambda p$  system [35]. However, this result should be considered with respect to the theoretical uncertainties of the Jost-function approach [40]. A direct determination of the spin singlet and triplet effective range parameters requires polarization measurements as proposed by Gasparyan et al. [41] and planned by COSY-ANKE and COSY-TOF.

## ACKNOWLEDGMENTS

The results presented here are due to the efforts of the collaborations COSY-ANKE, COSY-11, COSY-HIRES, COSY-MOMO and COSY-TOF and the COSY machine crew. The authors thank K.-Th. Brinkmann, H. Clement, W. Eyrich, H. Freiesleben, M. Hartmann, J. Ritman, E. Roderburg, M. Schulte-Wissermann, A. Sibirtsev, H. Ströher and Yu. Valdaу for their help and clarifying discussions.

## REFERENCES

1. R. Maier et al., *Nucl. Instr. and Meth. Phys. Res. Sect. A* **390**, 1 (1997).
2. M. Wolke, “Production of associated strangeness in the reaction  $pp \rightarrow ppK^+K^-$  close to threshold” *Jü1-3532* (1998).
3. C. Quentmeier et al., *Phys. Lett. B* **515**, 276 (2001) [arXiv:nucl-ex/0103001].
4. P. Winter et al., *Phys. Lett. B* **635**, 23 (2006) [arXiv:hep-ex/0602030].
5. M. Hartmann et al., *Phys. Rev. Lett.* **96**, 242301 (2006) *ibid.* **97**, 029901 (2006) [arXiv:hep-ex/0604010].
6. Y. Maeda et al., *Phys. Rev. C* **77**, 015204 (2008) [arXiv:0710.1755 (nucl-ex)].
7. V. Kleber et al., *Phys. Rev. Lett.* **91**, 172304 (2003) [arXiv:nucl-ex/0304020].
8. A. Dzyuba et al., *Eur. Phys. J. A* **29**, 245 (2006) [arXiv:nucl-ex/0605030].
9. Y. Maeda et al., *Phys. Rev. Lett.* **97**, 142301 (2006) [arXiv:nucl-ex/0607001].
10. Y. Maeda et al., *Phys. Rev. C* **79**, 018201 (2009) [arXiv:0811.4303 (nucl-ex)].
11. F. Belleman et al., *Phys. Rev. C* **75**, 015204 (2007) [arXiv:nucl-ex/0608047].
12. X. Yuan et al., *Eur. Phys. J. A* **42**, 1 (2009) [arXiv:0905.0979 (nucl-ex)].
13. F. Balestra et al., *Phys. Rev. C* **63**, 024004 (2001).
14. A. Dzyuba et al., *Phys. Lett. B* **668**, 315 (2008).
15. M. Silarski et al., *Phys. Rev. C* **80**, 045202 (2009).
16. M. Abdel-Bary et al., *Phys. Lett. B* **647**, 351 (2007) [arXiv:nucl-ex/0702059].
17. H.J. Lipkin, *Phys. Lett. B* **60**, 371 (1976).
18. K. Schönning et al., *Phys. Lett. B* **668**, 258 (2008).
19. S. Abd El-Samad et al., *Phys. Lett. B* **688**, 142 (2010).
20. A. Sibirtsev et al., *Eur. Phys. J. A* **27**, 269 (2006) [arXiv:nucl-th/0512059].
21. S. Abdel-Bary et al., *Eur. Phys. J. A* **46**, 27 (2010).
22. D. Grzonka and K. Kilian, *Nucl. Phys. A* **626**, 41C (1997).
23. J.T. Balewski et al., *Nucl. Phys. A* **626**, 85C (1997).
24. J.T. Balewski et al., *Phys. Lett. B* **420**, 211 (1998).
25. S. Severin et al., *Phys. Rev. Lett.* **83**, 682 (1999).
26. P. Kowina et al., *Eur. Phys. J. A* **22**, 293 (2004).
27. M. Abd El-Samad et al., *Phys. Lett. B* **632**, 27 (2006).
28. Yu. Valdaу et al., *Phys. Lett. B* **652**, 245 (2007) [arXiv:nucl-ex/0703044].
29. W.J. Fickinger et al., *Phys. Rev.* **125**, 2082 (1962).
30. A. Baldini et al., *Landolt-Börnstein*, New Series, I/12b (1988).
31. T. Rožek et al., *Phys. Lett. B* **643**, 251 (2006).
32. Yu. Valdaу et al., *Phys. Rev. C* **81**, 045208 (2010).
33. A. Budzanowski et al., *Phys. Lett. B* **692**, 10 (2010).
34. Yu. Valdaу and C. Wilkin, submitted to *Phys. Lett. B* (2010) [arXiv:1008.3465v1 (nucl-ex)].
35. A. Budzanowski et al., *Phys. Lett. B* **687**, 31 (2010).
36. M. Drochner et al., *Nucl. Phys. A* **643**, 55 (1998).
37. A.T.M. Aerts and C.B. Dover *Nucl. Phys. B* **253**, 116 (1985).
38. G. Alexander et al., *Phys. Rev.* **173**, 1452 (1968).
39. B. Sechi-Zorn et al., *Phys. Rev.* **175**, 1753 (1968).
40. A. Gasparyan et al., *Phys. Rev. C* **72**, 034006 (2005).
41. A. Gasparyan et al., *Phys. Rev. C* **69**, 034006 (2004).